

Orbital and Spin Frustration in the Shastry-Sutherland Lattice of DyB_4 Observed by Resonant X-ray Scattering

Daisuke Okuyama,* Takeshi Matsumura, Hironori Nakao, and Youichi Murakami
Department of Physics, Graduate School of Science, Tohoku University, Sendai 980-8578, Japan
(Dated: November 2, 2019)

We have observed geometrical frustration of quadrupolar and magnetic moments in dysprosium tetraboride, DyB_4 , where the rare-earth sites form a Shastry-Sutherland lattice. Resonant x-ray scattering at the L_{III} absorption edge of Dy was utilized. Analysis of the energy, polarization, temperature, and azimuthal-angle dependences of the $E1$ resonance of the $(1\ 0\ 0)$ forbidden reflection show that the magnetic and quadrupolar components within the frustrated c plane have a short-range correlation, suggesting that the moments are fluctuating. By contrast, the basic antiferromagnetic component along the c axis has a long-range order.

PACS numbers: 75.25.+z, 61.10.Eq, 71.20.Eh, 75.40.Cx

Magnetic materials with geometrically frustrated magnetic interactions exhibit a wide variety of intriguing phenomena caused by fluctuating spins that cannot order down to very low temperatures. For example, hexagonal ABX_3 (A=alkali metal, B=transition metal, X=halogen) compounds such as CsCoCl_3 with triangular lattice of Ising spins exhibit unusual antiferromagnetic state where one of the three sublattices is disordered [1]. Frustrations in kagomé and pyrochlore lattices offer a platform where a macroscopic number of spin configurations are degenerate, giving rise to short-range correlated fluctuating spins called a spin-liquid state [2]. These exotic phenomena are caused, of course, by the spin degree of freedom of the magnetic ions. On the other hand, very little is known about the frustration caused by the orbital degree of freedom. In this letter, we present new evidence for fluctuating orbital and spin moments in a rare-earth compound, DyB_4 , which has a Shastry-Sutherland-type geometrical frustration [3].

Rare-earth tetraborides, RB_4 , have been attracting growing interest as a system in which the rare-earth network involves a geometrical frustration. The R ions are at the $4g$ sites of the tetragonal space group of $P4/mbm$: $\mathbf{R}_1 = (x, x + \frac{1}{2}, 0)$, $\mathbf{R}_2 = (\frac{1}{2} - x, x, 0)$, $\mathbf{R}_3 = (-x, \frac{1}{2} - x, 0)$, and $\mathbf{R}_4 = (\frac{1}{2} + x, -x, 0)$, with $x = 0.3175$ for DyB_4 [4]. This is equivalent to the Shastry-Sutherland lattice as illustrated in the inset of Fig. 1 (b) [3]. It is noted that the nearest-neighbor and next nearest-neighbor distances differ only by 0.33% and that the Dy^{3+} ion has a huge magnetic moment of $10\mu_B$. Therefore, the Shastry-Sutherland lattice of Dy can be regarded as a combination of triangles and squares of classical moments. In addition, orbital degree of freedom is active in DyB_4 as described next. In these senses, the way of removing frustration in DyB_4 is expected to be different from the orthogonal dimer system of quantum spins such as $\text{SrCu}_2(\text{BO}_3)_2$, where the frustration can be removed by making spin-singlet dimers [5, 6].

Physical properties of DyB_4 have been studied intensively by Watanuki *et al* [4]. Two phase transitions take place at $T_{N1} = 20.3$ K and at $T_{N2} = 12.7$ K. Below T_{N1} , it is established by neutron powder diffraction that an antiferromagnetic order takes place with the magnetic moments align along the c axis; those on Dy(1) at \mathbf{R}_1 and Dy(2) at \mathbf{R}_2 direct upwards and those on Dy(3) at \mathbf{R}_3 and Dy(4) at \mathbf{R}_4 downwards. As a result, forbidden (odd $0\ 0$) reflections arise, but unit cell do not change. What is intriguing is that the C_{44} mode of the elastic constant keeps softening even below T_{N1} . The softening, which follows the normal Curie law in phase I ($T \geq T_{N1}$) indicating a quadrupolar degeneracy, is even more enhanced in phase II ($T_{N2} \leq T \leq T_{N1}$). Moreover, in phase II, strong ultrasonic attenuation occurs, suggesting fluctuation of the quadrupolar moments. Specific heat measurement shows that the entropy of $R \ln 2$ and $R \ln 4$ is released at T_{N2} and at T_{N1} , respectively, with increasing temperature. Therefore, the ground state is a pseudo-quartet with quadrupolar degeneracy, which is somehow not lifted even in phase II. In phase III ($T \leq T_{N2}$), the ultrasonic attenuation and softening stop; neutron powder diffraction suggests that a c -plane magnetic component arises in phase III. These anomalous behaviors strongly suggest that the phase II is not a normal antiferromagnetic state and that there remains fluctuating quadrupolar and magnetic moments.

In order to explore the phase II and III of DyB_4 , we have utilized resonant x-ray scattering (RXS), which has been developing as a powerful tool to probe both quadrupolar and magnetic moments [7]. Since RXS measures the average structure of the relevant moments in a very short time scale determined by the lifetime of the intermediate state ($\sim 10^{-15}$ sec), it would be possible to observe a snapshot of the correlated moments if the fluctuation rate is slower than the time scale of the observation.

The single crystal of DyB_4 was grown by the floating zone method using a high frequency furnace. The sample quality was checked by the magnetic susceptibility and electrical resistivity, which showed good agreements with the results in Ref. [4]. Synchrotron x-ray scattering

*Electronic address: oku@iijo.phys.tohoku.ac.jp

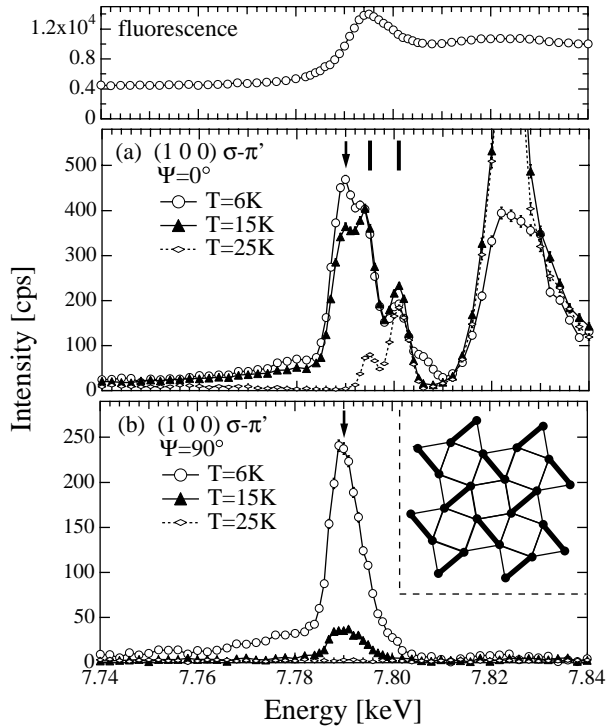


FIG. 1: Incident energy dependences of the peak-top intensity of the (1 0 0) reflection for σ - π' at (a) $\Psi = 0^\circ$ and (b) $\Psi = 90^\circ$. The peak around 7.824 keV for $\Psi = 0^\circ$ is due to the multiple scattering. Top figure shows the fluorescence spectrum. Inset shows the Dy lattice; the nearest neighbor bonds are shown by the thick lines.

experiments were performed using a four-circle diffractometer at the beamline BL-16A2 of the Photon Factory in KEK. Incident x-ray was tuned near the L_{III} absorption edge of Dy (~ 7.79 keV), where the resonance of $2p \leftrightarrow 5d$ dipole transition occurs. We investigated the $(h\ 0\ 0)$ reflections using a sample with the (100) surface. Azimuthal-angle scan and polarization analysis using a PG analyzer-crystal were also carried out; the azimuthal-angle Ψ is defined to be zero when the c axis lies in the scattering plane. The mosaic width of the sample was about 0.03° full width at half-maximum (FWHM) in phase I, indicating high quality of the crystal.

Figure 1 shows the incident energy dependences of the (1 0 0) forbidden reflection for the σ - π' channel at 6 K (phase III), 15 K (phase II), and 25 K (phase I) at two azimuthal angles of $\Psi = 0^\circ$ and 90° [8]. The resonant enhancement is clearly observed around the absorption edge. We notice three resonant features at $\Psi=0^\circ$ which are indicated by an arrow at 7.79 keV and two bars at 7.795 keV and 7.801 keV. The resonance at 7.79 keV, the inflection point of the fluorescence spectrum, disappears above T_{N1} ; this can be ascribed to the resonant exchange magnetic scattering originating from the 4f magnetic moment [9]. The other two resonances at 7.795 keV and 7.801 keV, which exist even above T_{N1} , can be

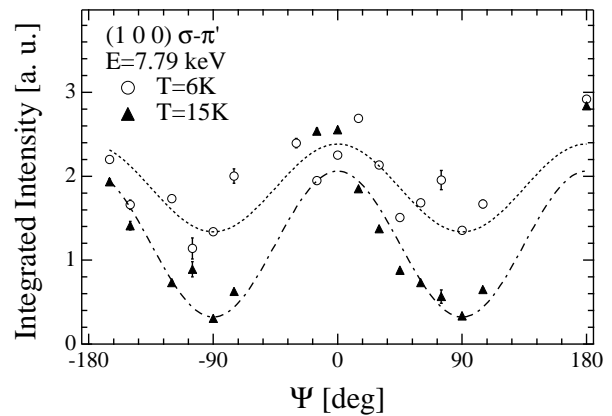


FIG. 2: Azimuthal-angle dependence of the integrated intensity of the (1 0 0) resonant reflection at $E = 7.79$ keV for σ - π' . Lines are the fits with $\cos^2 \Psi$ and $\sin^2 \Psi$.

ascribed to the anisotropic tensor susceptibility (ATS) scattering that reflect the local crystal-field anisotropy of the surrounding boron atoms. We call this as boron-ATS scattering hereafter. The double peak energy-spectrum and the $\cos^2 \Psi$ dependence in intensity are the same as those in GdB₄ [10, 11]. At $\Psi=90^\circ$, the boron-ATS scattering vanishes and only the resonance at 7.79 keV is observed as indicated by the arrow. We also observed nonresonant reflection below the edge, which we ascribe to magnetic scattering; the intensity is proportional to the resonance at 7.79 keV.

We note that the most mysterious point is the existence of the intensity at $\Psi=90^\circ$ in phase II. According to the simple magnetic structure deduced from neutron diffraction, where the antiferromagnetic moments align completely along the c axis, the structure factor of the resonant magnetic scattering becomes proportional to $\cos \Psi$. However, this is inconsistent with the data of Fig. 1 (b) for 15 K. The azimuthal-angle dependence of the resonance intensity shown in Fig. 2 also demonstrates that the intensity at $\Psi=90^\circ$ does not vanish in phase II. In phase III, a complex magnetic structure is proposed by neutron scattering, where the c -plane component of the magnetic moments appears [4]. It is therefore expected that the c -plane component gives the intensity at $\Psi=90^\circ$.

Figure 3 shows the temperature dependences of the integrated intensity and half width at half maximum (HWHM) of the (1 0 0) resonant reflection at 7.79 keV. There is an obvious difference between the behavior for $\Psi = 0^\circ$ and 90° . At $\Psi = 0^\circ$ the intensity rises up steeply below T_{N1} and saturates below about 17 K, whereas at $\Psi = 90^\circ$ it increases gradually below T_{N1} and exhibits a sudden increase below T_{N2} . Moreover, the HWHM at $\Psi = 90^\circ$ is obviously broad and exhibits a sudden drop below T_{N2} , whereas at $\Psi = 0^\circ$ it is almost resolution limited and exhibits slight broadening in phase II. It is noted that the rocking (ω) scans in Fig. 3 correspond to l -scan at $\Psi = 0^\circ$ and k -scan at $\Psi = 90^\circ$ in the hkl re-

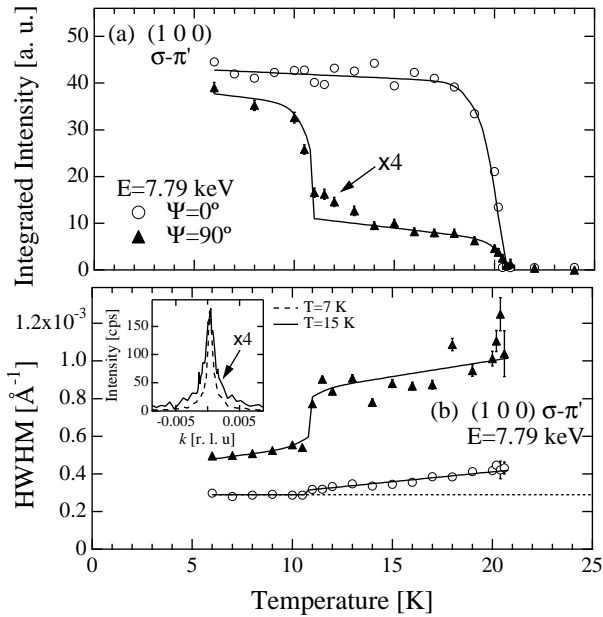


FIG. 3: Temperature dependences of (a) the integrated intensity and (b) the HWHM of the rocking scan (ω) of the (1 0 0) resonant reflection at $\Psi = 0^\circ$ and 90° ($E = 7.79$ keV, $\sigma\text{-}\pi'$). Solid lines are guides for eye. Dotted line indicates the resolution limit estimated from the fundamental reflections. Inset shows the peak profile at 7 K and 15 K for $\Psi = 90^\circ$.

ciprocal space. The HWHM for l -scan at $\Psi = 90^\circ$ is also obviously broader than the resolution, whereas that for k -scan at $\Psi = 0^\circ$ is resolution limited, although these resolutions are much worse because the scans correspond to the χ scan. These results suggest that a different order parameter exists at $\Psi=90^\circ$, which has a short correlation length in phase II.

We briefly refer to the structural phase transition in phase III that has been studied using an x-ray from Mo target (17.48 keV). The single peak of the (0 0 6) reflection at 16 K splits into four peaks along the h and k directions at 9 K; the (10 0 0) peak becomes broad along the l direction. These results, together with the survey of some other Bragg peaks, show that the structure changes from tetragonal to monoclinic. The angle $\angle ac$, or $\angle bc$, is estimated to be 89.84° at 9 K. It should be remarked that the antiferromagnetic domain with the (1 0 0) and (0 1 0) propagation vector results in the monoclinic distortion within the bc plane ($\angle bc \neq 90^\circ$) and the ac plane ($\angle ac \neq 90^\circ$), respectively; this is inferred from the fact that the (1 0 2) resonant magnetic Bragg peak splits only along the k direction in phase III.

Let us discuss the origin of the nonzero intensity of the (1 0 0) resonant reflection at $\Psi = 90^\circ$ in phase II. We analyze the RXS result by taking into account the c -plane components of both magnetic (rank 1) and quadrupolar (rank 2) moments. For this purpose we use a theory developed by Lovesey *et al.* which directly connects the

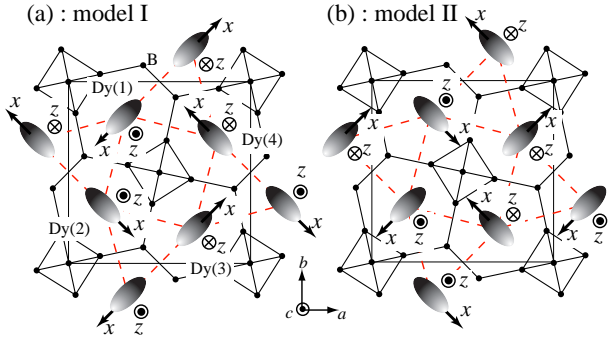


FIG. 4: Models of possible magnetic and quadrupolar structures. The local x and z axis corresponds to the c -plane and c -axis magnetic component of each Dy ion, respectively. Ellipses with light and dark shade represent $\langle O_{zx} \rangle$ -type charge distributions that is extended above and below the paper, respectively.

atomic tensors to the scattering amplitude of RXS [7, 12].

Here, we examine two possible models of the in-plane magnetic and quadrupolar structures that are consistent with the experimental results. They are illustrated in Fig. 4. We take the direction of the c -plane and c -axis component as the local x and z axis, respectively. The atomic tensors expressed in the local xyz coordinates are assumed to be the same for all the four Dy ions; they can be transformed to each other by appropriate Euler rotations. Quadrupolar moments represented by the ellipses can coexist because of the strong spin-orbit interaction.

The unit cell structure factor of the ($h=$ odd 0 0) reflection for the two models in Fig. 4 is written as

$$F_{\sigma\text{-}\pi'}^{(E1)} = 2k_1 b \cos \theta (\sqrt{2} \langle J_z \rangle \cos \Psi - \langle J_x \rangle \sin \Psi) \\ \mp 2k_2 a \cos \theta (\sqrt{2} \langle O_{22} \rangle \cos \Psi + \langle O_{zx} \rangle \sin \Psi) \quad (1)$$

for $E1$ resonance and $\sigma\text{-}\pi'$ channel, where the minus sign in the second line corresponds to model I and plus sign to model II; $a = \cos(2\pi h x)$ and $b = \sin(2\pi h x)$; θ is the Bragg angle; k_1 and k_2 are constant real numbers, respectively. Note that the tensors in Eq. (1) are of the 5d state; $\langle J_\alpha \rangle$ can be induced through magnetic exchange interaction with $\langle J_\alpha \rangle_{4f}$; $\langle O_\gamma \rangle$ through $d\text{-}f$ Coulomb interaction with $\langle O_\gamma \rangle_{4f}$ or through mixing with the 2p orbitals of boron atoms (boron-ATS mechanism)[7]. The boron-ATS mechanism obviously gives rise to $\langle O_{22} \rangle$, and this term explains the azimuthal-angle dependences of the resonance at 7.795 keV and 7.801 keV in phase I. In phase II, the c -axis component of the 4f magnetic moment induces $\langle J_z \rangle$. The $\langle J_z \rangle$ term explains the $\cos^2 \Psi$ component in the azimuthal-angle dependence of the resonance at 7.79 keV as shown in Fig. 2.

The $\langle J_x \rangle$ and $\langle O_{zx} \rangle$ terms, with the $\sin \Psi$ dependence, can explain the nonzero intensity at $\Psi=90^\circ$. However, because the $\cos \Psi$ and $\sin \Psi$ terms interfere coherently in Eq. (1), the structure factor can be transformed into the form $A \cos(\Psi + \alpha)$, where A and α is a constant.

This means that the intensity must vanish somewhere in the azimuthal scan, which is the case in GdB_4 [10]. However, the experimental data in Fig. 2 do not support this simple scenario. The data suggest that the $\cos \Psi$ term and the $\sin \Psi$ term contribute independently rather than they interfere coherently. This is demonstrated by the lines in Fig. 2. It seems that the resonance at $\Psi = 90^\circ$ represents the in-plane components of $\langle J_x \rangle$ and $\langle O_{zx} \rangle$, and the resonance at $\Psi = 0^\circ$ represents the $\langle J_z \rangle$ and $\langle O_{22} \rangle$ moments, respectively.

A possible reason for this behavior is that the correlation length of $\langle J_x \rangle$ and $\langle O_{zx} \rangle$ components are much shorter than that of $\langle J_z \rangle$ and $\langle O_{22} \rangle$. By fitting the k -scan profile at $\Psi = 90^\circ$ with a Lorentzian that is convoluted with the resolution function, the correlation length of $\langle J_x \rangle$ and $\langle O_{zx} \rangle$ along the b axis is estimated to be $(1.4 \pm 0.1) \times 10^3 \text{ \AA}$ at 15 K in phase II and $(4.2 \pm 0.2) \times 10^3 \text{ \AA}$ at 7 K in phase III. The correlation along the c axis is also short as well, less than the resolution of $1.5 \times 10^3 \text{ \AA}$ although precise estimation was difficult. On the other hand, the correlation of $\langle J_z \rangle$ and $\langle O_{22} \rangle$ along the c axis estimated from the l -scan profile at $\Psi = 0^\circ$ is $(9.2 \pm 0.5) \times 10^3 \text{ \AA}$ at 15 K and over $2 \times 10^4 \text{ \AA}$, the resolution limit, at 7 K. The correlation along the b axis is also expected to be longer than the resolution limit of $1.5 \times 10^3 \text{ \AA}$. Then, the volume fraction from which the scattering occurs coherently is much smaller for $\langle J_x \rangle$ and $\langle O_{zx} \rangle$ than for $\langle J_z \rangle$ and $\langle O_{22} \rangle$. Therefore, $\cos \Psi$ and $\sin \Psi$ terms in Eq. (1) can hardly interfere and they give reflections independently.

Thus, we consider that the resonance at $\Psi = 90^\circ$ observes $\langle J_x \rangle$ or $\langle O_{zx} \rangle$, which is induced by the magnetic and quadrupolar moments of the $4f$ electrons, respectively. The peak profiles are clearly broadened in phase II, indicating that the correlation length is short. Furthermore, these in-plane components are considered to be fluctuating. This is supported by neutron powder diffraction in phase II, which shows that $\langle gJ_z \rangle_{4f}$ is only $6.9 \mu_B$ while the full moment is $10 \mu_B$. The strong ultrasonic attenuation in the C_{44} mode also supports the fluctuation of $\langle O_{zx} \rangle$ [4]. In phase III, neutron diffraction shows that the in-plane component of $5.3 \mu_B$ appears, resulting in the total moment of $8.8 \mu_B$; the ultrasonic attenuation and softening also stops. RXS at $\Psi=90^\circ$ shows that the correlation length becomes longer, although it is not as long as the resolution limit. These results show that the fluctuation stops in phase III and a static short-range order of $\langle J_x \rangle$ and $\langle O_{zx} \rangle$ remains.

Which of $\langle J_x \rangle$ and $\langle O_{zx} \rangle$ is dominant in this reflection? Unfortunately, it is not distinguishable from the present experimental results and from Eq. (1) because the two factors are completely in phase. In the present case of

DyB_4 , because $\langle J_z \rangle$ is finite, $\langle O_{zx} \rangle$ will be induced if $\langle J_x \rangle$ arises because of the strong spin-orbit coupling, and $\langle J_x \rangle$ will be induced if $\langle O_{zx} \rangle$ arises as well. Ultrasonic attenuation and softening of the C_{44} mode seem to support the dominance of $\langle O_{zx} \rangle$. It would be possible to distinguish if we could investigate by RXS the relative change in the signal for $h=1, 3$, and 5 of the $(h 0 0)$ reflection through the change in the factors of a and b , which have different h dependences.

With respect to the origin of the short-range correlation and fluctuation of the in-plane moment, one plausible scenario is that the $\langle O_{zx} \rangle$ moments in the triangular connection of the Dy lattice possess frustration. If we assume the charge distribution of the $4f$ electrons prefer to avoid each other, the arrangement of $\langle O_{zx} \rangle$ in models I and II experiences frustration, which could lead to an orbital liquid state.

We consider that the static order of the in-plane moments takes place when the frustration is removed by the lattice distortion. The arrangement of the $\langle O_{zx} \rangle$ -type quadrupolar moment in models I and II will favor a uniform lattice distortion through cooperative Jahn-Teller effect into a monoclinic structure where the bc plane is distorted ($\angle bc \neq 90^\circ$). This is consistent with the experimental result in phase III. A possible space group of the monoclinic phase allowed by Landau theory is $P2_1/c$, where all the atomic sites are described by the $4e$ site [13]. It is intriguing that the peak width at $\Psi = 90^\circ$ is still broader than the resolution limit, which means that the correlation length does not diverge.

In summary, we have investigated the phase transitions occurring in the Shastry-Sutherland lattice of DyB_4 by resonant x-ray scattering, and detected the short-range correlated in-plane moments of $\langle J_x \rangle$ and $\langle O_{zx} \rangle$. They are expected to be fluctuating in the high-temperature antiferromagnetic phase because of frustration and they change into a static order with short-range correlation in the low-temperature phase with monoclinic distortion. However, the fundamental problem has not yet been solved; what is the doublet that remains even after the c -axis component of the magnetic moment is fixed below T_{N1} ?

The authors are indebted to R. Watanuki for many fruitful discussions. We also thank S. Kunii, K. Horiochi, M. Onodera, H. Shida for helping single crystal growth, Y. Wakabayashi for experimental supports, K. Iwasa, K. Suzuki for profitable discussions. This study was performed under the approval of the Photon Factory Program Advisory Committee (No. 2004G235), and was supported by the 21st century center of excellence program, and by a Grant-in-Aid for Scientific Research from the Japanese Society for the Promotion of Science.

[1] M. Mekata, J. Phys. Soc. Jpn. **42**, 76 (1977).
[2] I. Mirebeau and I. N. Goncharenko, J. Phys. Condens. Matter **17**, S771 (2005).

[3] B. S. Shastry and B. Sutherland, Physica (Amsterdam) **108B**, 1069 (1981).
[4] R. Watanuki, Ph.D. thesis, Yokohama National Univer-

sity, 2004.

[5] H. Kageyama, K. Yoshimura, R. Stern, N. V. Moshnikov, K. Onizuka, M. Kato, K. Kosuge, C. P. Slichter, T. Goto, and Y. Ueda, Phys. Rev. Lett. **82**, 3168 (1999).

[6] Shin Miyahara and Kazuo Ueda, Phys. Rev. Lett. **82**, 3701 (1999).

[7] T. Matsumura, D. Okuyama, N. Oumi, K. Hirota, H. Nakao, Y. Murakami, and Y. Wakabayashi, Phys. Rev. B **71**, 012405 (2005).

[8] No reflection was observed for σ - σ' at any azimuthal angle.

[9] J. P. Hannon, G. T. Trammell, M. Blume, and D. Gibbs, Phys. Rev. Lett. **61**, 1245 (1988) [Errata, **62**, 2644 (1989)].

[10] S. Ji, C. Song, J. Koo, K.-B. Lee, Y. J. Park, J. Y. Kim, J.-H. Park, H. J. Shin, J. S. Rhyee, B. H. Oh, and B. K. Cho, Phys. Rev. Lett. **91**, 257205 (2003).

[11] S. W. Lovesey, J. Fernández Rodríguez, J. A. Blanco, P. J. Brown, Phys. Rev. B **70**, 172414 (2004).

[12] S. W. Lovesey, and K. S. Knight, Phys. Rev. B **64**, 094401 (2001).

[13] H. T. Stokes and D. M. Hatch, *Isotropy Subgroups of the 230 Crystallographic Space Groups* (World Scientific, 1988).